Published online May 16, 2007

An Improved Approach for Measurement of Coupled Heat and Water Transfer in Soil Cells

J. L. Heitman*
R. Horton
Dep. of Agronomy
Iowa State Univ.
Ames, IA 50011

T. Ren
Dep. of Soil and Water
China Agricultural Univ.
Beijing 100094 China

T. E. Ochsner
USDA-ARS
Univ. of Minnesota
1991 Buford Cir.
St. Paul, MN 55108

Laboratory experiments on coupled heat and water transfer in soil have been limited in their measurement approaches. Inadequate temperature control creates undesired two-dimensional distributions of both temperature and moisture. Destructive sampling to determine soil volumetric water content (θ) prevents measurement of transient θ distributions and provides no direct information on soil thermal properties. The objectives of this work were to: (i) develop an instrumented closed soil cell that provides one-dimensional conditions and permits in situ measurement of temperature, θ, and thermal conductivity (λ) under transient boundary conditions, and (ii) test this cell in a series of experiments using four soil type–initial θ combinations and 10 transient boundary conditions. Experiments were conducted using soil-insulated cells instrumented with thermo-time domain reflectometry (T-TDR) sensors. Temperature distributions measured in the experiments show nonlinearity, which is consistent with nonuniform thermal properties provided by thermal moisture distribution but differs from previous studies lacking one-dimensional temperature control. The T-TDR measurements of θ based on dielectric permittivity, volumetric heat capacity, and change in volumetric heat capacity agreed well with post-experiment sampling, providing r^2 values of 0.87, 0.93, and 0.95, respectively. Measurements of θ and λ were also consistent with the shapes of the observed temperature distributions. Techniques implemented in these experiments allowed observation of transient temperature, θ, and λ distributions on the same soil sample for 10 sequentially imposed boundary conditions, including periods of rapid redistribution. This work demonstrates that, through improved measurement techniques, the study of heat and water transfer processes can be expanded in ways previously unavailable.

Abbreviations: TDR, time domain reflectometry; T-TDR, thermo-time domain reflectometry.

Thermal gradients drive soil heat and water transfers. Heat and water transfers, in turn, create transient temperature, water content, and thermal conductivity distributions. Heat and water transfer is a coupled process important for unsaturated, near-surface conditions. Yet our understanding of this process has been limited by a lack of thorough experimental testing. To date, laboratory data on temperature distributions for coupled heat and water transfer have been collected, but undesired two-dimensional distributions of both temperature and water often occur, which limits comparison and analysis (Prunty and Horton, 1994). Laboratory data on θ has most commonly been obtained through destructive sampling (cf. Nassar and Horton, 1989), which prevents measurement of transient conditions and precludes the possibility of applying more than one set of boundary conditions to a given sample. These limitations restrict testing and refinement of coupled heat and water transfer theory. Evaluation of the dominant transfer theories has been limited primarily to model calibration against steady-state moisture and temperature distributions. Attempts at validating the calibrated model or at describing transient boundary conditions are sorely lacking.

There are a few reports of in situ measurement of θ using time domain reflectometry (TDR) to study coupled heat and water transfer (cf. Cahill and Parlange, 1998); however, TDR does not provide measurement of soil thermal properties or temperature. Thus, existing measurement approaches can lead to difficulty in interpretation of experimental results or prevent measurement of transient temperature, moisture redistribution, and thermal properties. Recent improvements in temperature control (Zhou et al., 2006) and in situ measurement of both θ and soil thermal properties (Ren et al., 2005) can overcome these limitations and provide new opportunities for investigation of coupled heat and moisture transfer in laboratory experiments.

Prunty and Horton (1994) recognized that laboratory experiments aimed at one-dimensional thermal and moisture redistribution were often affected by ambient temperature conditions. Two-dimensional distributions of both moisture and temperature result from the combined effect of imposed temperature conditions and ambient temperature interference. These two-dimensional conditions may provide linear or even convex (i.e., steepest temperature gradients near the cool end) temperature distributions between boundaries, which differ significantly from theoretical description and modeling efforts (e.g., Bach, 1992). When this interference is removed, temperature distributions typically become concave, because one-dimensional moisture redistribution results in non-

Soil Sci. Soc. Am. J. 71:872–880
doi:10.2136/sssaj2006.0327
Received 15 Sept. 2006.
*Corresponding author (jheitman@iastate.edu).

uniform thermal properties. Zhou et al. (2006) made use of this thermal moisture redistribution to provide one-dimensional temperature conditions in their experiments. They insulated a closed-cell control volume with a concentric layer of similar soil material. Allowing thermal moisture redistribution in both the control volume and the insulation provides a close match in thermal properties, and thereby reduces ambient temperature interference on the control volume. With this new column design, Zhou et al. (2006) were able to achieve a ratio of 1:0.02 between imposed axial and ambient radial temperature distributions, thus effectively providing one-dimensional conditions.

Recently developed instrumentation for in situ measurement of θ has successfully made use of both TDR (Topp et al., 1980) and the heat-pulse method (Campbell et al., 1991). Time domain reflectometry uses calibration of the relationship between soil dielectric permittivity and θ, whereas the heat-pulse method uses the linear relationship between soil volumetric heat capacity and θ. The TDR sensors are typically larger than heat-pulse sensors, but building on Noborio et al. (1996), Ren et al. (1999, 2003a) combined both measurement techniques in a single sensor, termed a T-TDR sensor. The small size of T-TDR sensors makes them ideal for measurement within a soil cell during laboratory experiments. Their dual function provides independent, colocated estimates of θ, as well as measurement of λ via the heat-pulse method (Bristow et al., 1994).

Ren et al. (2005) evaluated both TDR and the heat-pulse techniques implemented with the T-TDR sensor for measurement of θ. They found that both techniques provided measurement volumes approximately representing cylinders with a radius <1.5 cm around the center of the probe, thus providing fine spatial resolution. Both techniques also provided accurate measurement of θ with RMSE of 0.023 and 0.022 $m^3\ m^{-3}$ for the TDR and heat-pulse techniques, respectively, across a range in θ of 0.04 to 0.30 $m^3\ m^{-3}$. Ren et al. (2003b) noted that the heat-pulse technique accuracy could be improved when the heat-pulse method was used to establish the specific heat of the solid soil component. Other researchers have used the heat-pulse method for determining the change in volumetric water content (Δθ), thereby eliminating the need for estimation of soil specific heat (Bristow et al., 1993). Basinger et al. (2003) evaluated this approach. They found that the heat-pulse approach for measuring Δθ provided accurate measurements (RMSE = 0.012 $m^3\ m^{-3}$) for a range in Δθ of 0 to 0.35 $m^3\ m^{-3}$.

Implementation of both one-dimensional temperature control and in situ measurement with T-TDR sensors provides new opportunities for studying coupled heat and water transfer in the laboratory. It offers the opportunity to expand on previous laboratory experiments, which consider only simple boundary and initial conditions. It also offers the opportunity to collect complete data sets for transient temperature, θ, and λ distributions, which to our knowledge do not currently exist. Therefore, the objectives of this work were to: (i) develop an instrumented soil column that provides one-dimensional conditions with in situ measurement of temperature, θ, and λ, under transient boundary conditions, and (ii) test the utility of this column through a series of transient experiments. For these experiments, we considered two soil types and four initial moisture contents (two per soil) under a series of 10 imposed boundary temperature conditions.

Table 1. Particle-size analysis and organic matter content of the soils used in this study.

Soil material	Textural fractions: Sand >50 μm	Coarse silt 50–20 μm	Fine silt 20–2 μm	Clay <2 μm	Organic matter
	%				
Sand	91.7†	5.0	2.2	1.1	0.6
Silt loam	2.2	42.9	30.0	24.9	4.4

† The sand fraction had 0.2, 14.7, 79.7, and 5.3% in the size ranges 1000–500, 500–250, 250–106, and 105–50 mm, respectively.

MATERIALS AND METHODS

Soil Materials

Two soil materials of differing texture were used in the experiments, sand and silt loam. The sand was collected from the subsurface of a Hanlon sand (coarse-loamy, mixed, superactive, mesic Cumulic Hapludoll) map unit delineation near Ames, IA. The silt loam was collected from the surface horizon of an Ida silt loam (fine-silty, mixed, superactive, calcareous, mesic Typic Udorthent) delineation near Treynor, IA. The soil samples were air dried, passed through a 2-mm sieve, and homogenized. Particle-size analysis was conducted with the pipette method (Soil Survey Staff, 1972), and organic matter content was determined by combustion (Table 1). Water-characteristic curves were measured for the soils using pressure cells (Dane and Hopmans, 2002a), pressure plate extractors (Dane and Hopmans, 2002b), and a WP4 DewPoint Potentiometer (Decagon Devices, Pullman, WA) in the matric potential ranges of greater than −20, −20 to −1500, and less than −1500 kPa, respectively (Fig. 1).

Two different initial moisture contents (θ_o), chosen to provide a range of conditions, were used for each soil in the experiments, giving a total of four soil–θ_0 combinations: sand at θ_o = 0.08 and 0.18 $m^3\ m^{-3}$ and silt loam at θ_o = 0.10 and 0.20 $m^3\ m^{-3}$ (hereafter referred to as s-8, s-18, sil-10, and sil-20, respectively). The soils were wetted with 0.005 *M* $CaCl_2$ to achieve the desired θ_o and then packed into soil cells in 2-cm depth increments to uniform bulk densities of 1.6 and 1.2 Mg m^{-3} for the sand and silt loam, respectively.

Soil Cells

The soil cells were identical to the short, wide cell used by Zhou et al. (2006). The cell consisted of a smaller soil column (10-cm length, 8.9-cm inside diameter) surrounded by a larger soil column (20.2-cm inside diameter) of the same length (Fig. 2). The columns were made

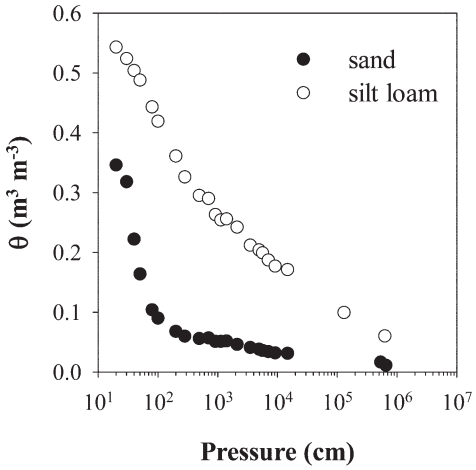

Fig. 1. Water characteristic curves for the experimental soils (θ = water content).

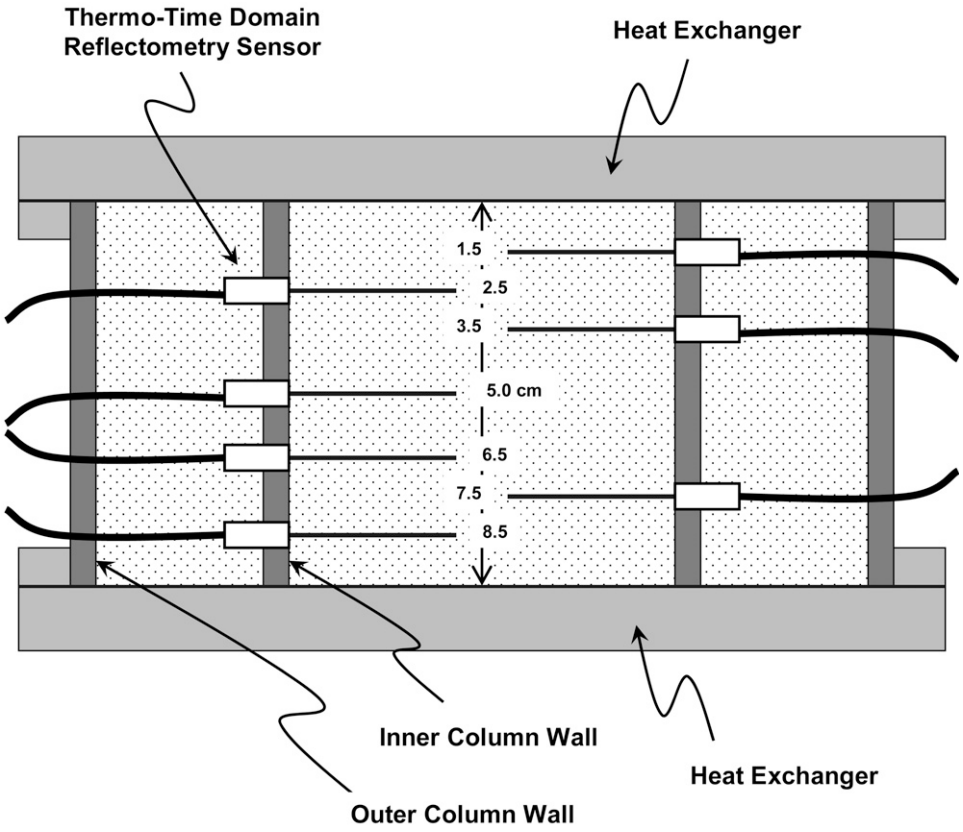

Fig. 2. The closed soil cell. The diagram represents a cross-section of the closed soil drawn approximately to scale.

from Schedule 40 polyvinyl chloride pipe. Both soil columns were packed with identical soil material so that the smaller soil column served as an isolated control volume and the larger column served as a concentric insulation layer. An additional concentric layer of fiberglass pipe insulation of 3.8-cm thickness was placed around the cells during the experiments to further limit ambient temperature effects.

The ends of the cells were closed with spiral circulation heat exchangers, consisting of a spiral loop for fluid circulation and a Cu heat-exchange plate enclosed in Plexiglas. Details of the design for the heat exchangers are given in Zhou et al. (2006). Temperature at the heat exchangers was controlled by circulating water from water baths (Programmable Digital Circulator, Model 9512, PolyScience, Niles, IL). The entire assembled cells were placed in a temperature-controlled room with room temperature set at 22°C for the experiment duration.

Instrumentation

The T-TDR sensors were built following the design of Ren et al. (2003a). The sensors consist of three stainless steel needles held at one end in an epoxy body. Each needle is 0.0013 m in diameter and 0.04 m in length. Sensor needles are positioned in parallel, with 0.06-m spacing between adjacent needles. The outer sensor needles contain 40-gauge Type E (chromel-constantan) thermocouples for measuring temperature. The inner sensor needle contains a resistance heater (resistance = 533 Ω m^{-1}) for producing the slight temperature perturbation required in the heat-pulse method. For the TDR function of the sensor, the center conductor of a coaxial cable (75 Ω) is soldered to the center needle and the shield of the cable is split and soldered to the two outer needles.

Each cell included seven T-TDR sensors at positions of 1.5, 2.5, 3.5, 5.0, 6.5, 7.5, and 8.5 cm along the axis of the cell (Fig. 2). The sensors were installed on alternate sides of the cell through ports in the inner column wall after the column had been packed with soil. Installation was accomplished by pushing the needles into the soil such that the plane of the needles was perpendicular to the axis of the cells and only the sensor needles were within the soil of the inner column. After installation, the sensor leads were routed through additional ports in the outer column of the cells to the data acquisition system (discussed below). The space around the sensor leads in the installation ports was sealed with putty. The outer column was then packed with soil in 2-cm depth increments to match the bulk density of the inner column.

The T-TDR sensors were used for three functions: temperature, heat-pulse, and TDR measurements. For temperature measurements, the thermocouples of the outer needles were connected via multiplexers (Model AM16/32, Campbell Scientific, Logan, UT) to a datalogger (Model CR23X, Campell Scientific). The connection between the multiplexers and the datalogger was made using insulated thermocouple wire (Type E, 40 gauge); the datalogger panel temperature was used as the reference temperature. Heat-pulse measurements made use of these thermocouples, but also used a heater-control relay circuit connected to the sensor middle needle. The heater-control relay circuit consisted of a 12-V DC power supply controlled by a relay with the datalogger and a 1-Ω precision resistor. Heaters were multiplexed with AM416 multiplexers (Cambell Scientific). Heat-pulse measurements consisted of a 100-s sequence (1-s measurement interval) including 6-s background temperature measurement and 8-s heating ($\sim$60 W m^{-1}). Heat inputs were inferred from the measured voltage drop across the precision resistor. The apparent distance between the heater of each sensor and the thermocouples of the outer needles was determined by calibration in 6 g L^{-1} agar stabilized water (Campbell et al., 1991). Volumetric heat capacity (C, J m^{-1} °C^{-1}), thermal diffusivity (m^2 s^{-1}), and λ (W m^{-1} °C^{-1}) were calculated from the measured temperature response curves using the HPC code (Welch et al., 1996). The three-needle T-TDR design provides two measurements of thermal properties per heating of each sensor.

The TDR measurements were made using a cable tester (Model 1502C, Tektronix Inc., Beaverton, OR) with T-TDR sensors connected via multiplexers (Model SDMX50, Campbell Scientific) to a computer. Waveform analysis was accomplished with the WinTDR package (Or et al., 1998). The apparent length of the T-TDR probes (L_a) was determined following the procedure of Ren et al. (2005) using measurements in air and distilled water. Subsequently, the relative dielectric permittivity (K_a) from experimental measurements was determined according to

$$K_a = \left(\frac{L_2 - L_1}{L_a} \right)^2 \qquad [1]$$

where L_1 and L_2 are the initial and end reflection points, respectively.

Four soil cells were operated concurrently, thus 28 T-TDR sensors were connected to the data acquisition system. Thermocouples in the outer needles of the T-TDR sensors were used to collect hourly temperature measurements. Two additional thermocouples were used in each cell to measure the cell end temperatures at the soil–heat exchanger interface. The T-TDR sensors were used to collect heat-pulse and TDR measurements once every 4 h.

Soil Water Content Estimation

Three methods were used for estimation of θ from the T-TDR measurements. The TDR function of the sensor was used to calculate θ from K_a. We applied the Topp equation (Topp et al., 1980) to estimate TDR soil water content (θ_{TDR}):

$$\theta_{TDR} = -5.3\times10^{-2} + 2.92\times10^{-2}K_a - 5.5\times10^{-4}K_a^2 + 4.3\times10^{-6}K_a^3 \quad [2]$$

We used two additional approaches to estimate θ based on the heat-pulse method. In the first approach, the heat-pulse water content (θ_{HP}) was calculated from C according to (Campbell et al., 1991)

$$\theta_{HP} = (C - \rho_b c_s)/C_w \quad [3]$$

where ρ_b (Mg m^{-3}) is the soil bulk density and C_w is the volumetric heat capacity of water (4.18 MJ m^{-3} °C^{-1}). The specific heat of the solid constituents (c_s, J g^{-1} C^{-1}) was estimated from

$$c_s = c_m\phi_m + c_o\phi_o \quad [4]$$

where c_m and c_o are the specific heat of the mineral and organic components, respectively, and ϕ_m and ϕ_o are the mass fraction of the mineral and organic components, respectively. Values of 0.73 and 1.9 kJ kg^{-1} °C^{-1} were used for c_m and c_o, respectively (Kluitenberg, 2002).

The second estimate from the heat-pulse method was based on the Δθ approach of Bristow et al. (1993). The change in water content was computed according to

$$\Delta\theta = (C_i - C_o)/C_w \quad [5]$$

where the subscripts o and *i* refer to the initial heat-pulse reading and the *i*th reading taken at some later time, respectively. By assuming that the initial condition in the experiment was a uniform moisture distribution, computation of Δθ and subsequent addition of θ_o allowed calculation of an additional estimate of θ based on the heat-pulse method ($\theta_{HP,\Delta}$), which was independent of c_s:

$$\theta_{HP,\Delta} = \theta_o + \Delta\theta \quad [6]$$

Temperature Conditions

A series of one-dimensional temperature boundary conditions was imposed on the four cells simultaneously. The first temperature series consisted of three mean temperatures with three temperature gradients imposed around each mean, for a total of nine temperature combinations: mean temperature = 15, 22.5, and 30°C; temperature gradient = 50, 100, and 150°C m^{-1} (warm end vertically upward). Following these temperature conditions, the 22.5°C mean temperature was again tested with the direction of the 100°C m^{-1} gradient reversed. Each of these 10 constant-boundary temperature gradients was imposed for approximately 96 h before moving immediately to the next temperature condition. The 96-h time period was chosen to achieve steady-state temperature conditions, although not necessarily steady-state moisture distributions. Temperature measurements collected each hour were used to test if this steady-state temperature condition was met. Results indicate that the average deviation in temperature at a given measurement position during the last 12 h of each constant-boundary temperature condition was 0.02°C.

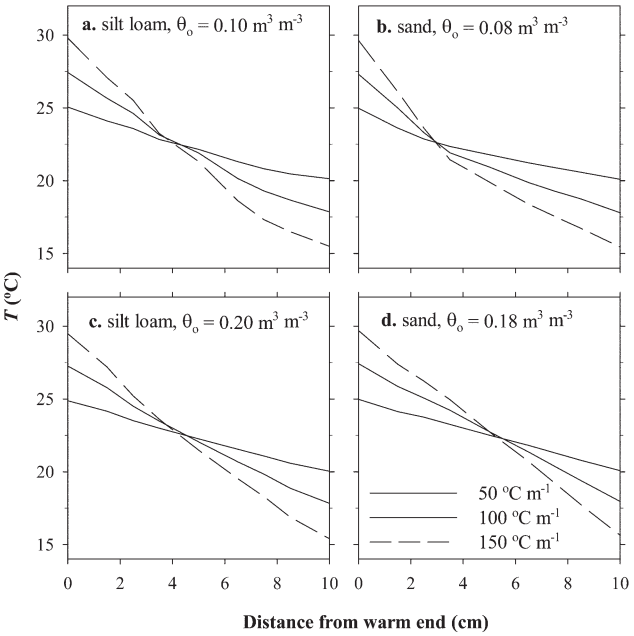

Fig. 3. Steady-state temperature (*T*) distributions at 22.5°C gradient mean temperature. Lines represent temperature distributions obtained after 96-h application of imposed temperature gradients (θ_o = initial water contents).

Post-Experiment Sampling

At the experiment conclusion, soil cells were allowed to re-equilibrate for 96 h at a uniform imposed temperature of 22.5°C. This step was taken before disassembly to avoid rapid water redistribution when imposed temperature gradients were removed. Final heat-pulse and TDR measurements were collected for all cells and depths just before disassembly. Cells were then disassembled, with both the inner and outer columns sectioned into 1-cm depth increments. These samples were weighed, dried for 24 h at 105°C, and reweighed to determine θ.

RESULTS AND DISCUSSION

Steady-State Temperature Distributions

Steady-state temperature distributions for gradient mean temperature = 22.5°C and each soil–θ_o combination are shown in Fig. 3. Nonlinearity, specifically concavity, in the temperature distributions is apparent for both the silt loam and the sand at the lower θ_o (Fig. 3a and 3b). Concavity is indicative of nonuniform thermal properties within the cells (Prunty and Horton, 1994). This concavity increased with the temperature gradient magnitude. The differential in boundary temperatures drove a net water flux to the cold end, which increased the thermal conductivity and correspondingly decreased the thermal conductivity of the warm end. This resulted in a steeper thermal gradient near the warm end.

Temperature distributions for both soils at the higher θ_o appear nearly linear (Fig. 3c and 3d). Concavity can also be observed to a lesser extent, however, for sil-20 under the 100 and 150°C m^{-1} temperature gradients by noting that the gradient mean temperature (22.5°C) is reached at a position 4 cm along the column, which is nearer to the warm end (Fig. 3c).

The 100°C m^{-1} temperature gradient for each soil–θ_o combination under each of the three mean gradient temperatures is shown in Fig. 4. The shape of these temperature distributions was consistently linear for s-18 (Fig. 4d), but varied by mean temperature for the remaining three cells (Fig. 4a–4c). In these cells, concavity is most distinct at the 30°C mean temperature, but the inflection point of the temperature distribution is similarly located at each mean temperature. As before, this concavity indicates nonuniformity of thermal properties, which increased with mean temperature.

Thermo-Time Domain Reflectometry Estimated Water Contents

All cells were disassembled and sectioned to determine final θ. The results of this sampling for both the inner and outer columns of each cell indicate an average loss of <0.01 m^3 m^{-3} from the initial condition. This water loss probably represents water evaporated during column packing or post-experiment sampling and is consistent with, or slightly better than, water recovery reported in the closed-cell experiments of Zhou et al. (2006) and Prunty and Horton (1994).

Post-experiment sampling provided an opportunity to test various methods for computing θ from T-TDR measurements. Each heat-pulse measurement provided two estimates of C, which were averaged for calculation of θ_{HP} and $\theta_{HP,\Delta}$. Regression analyses of θ_{TDR}, θ_{HP}, and $\theta_{HP,\Delta}$ vs. gravimetric samples collected at the ends of the experiments are shown in Fig. 5. The regression relationships for θ_{TDR} and θ_{HP} were similar to those reported by Ren et al. (2005). Both methods provided RMSE ≤0.02 m^3 m^{-3}, but θ_{TDR} provided a slightly smaller slope and slightly larger intercept than those observed by Ren et al. (2005). One possible explanation for the overestimate for the lower θ range with TDR is the empirical nature of the function (Eq. [2]) used to describe the relationship between K_a and θ. Separating the silt loam and sand for regression resulted in similar regression slopes (~0.95) and improved regression relationships (r^2 = 0.94 and 0.97, respectively), but with distinctly different intercepts of −0.01 and 0.02, respectively. Maximum θ for the sand sample was ≤0.20 m^3 m^{-3}, which results in a smaller slope for the pooled regression relationship.

For the heat-pulse method, calculation of θ from the measurements was further improved using $\theta_{HP,\Delta}$ (Fig. 5). As mentioned above, this approach removes the need for estima-

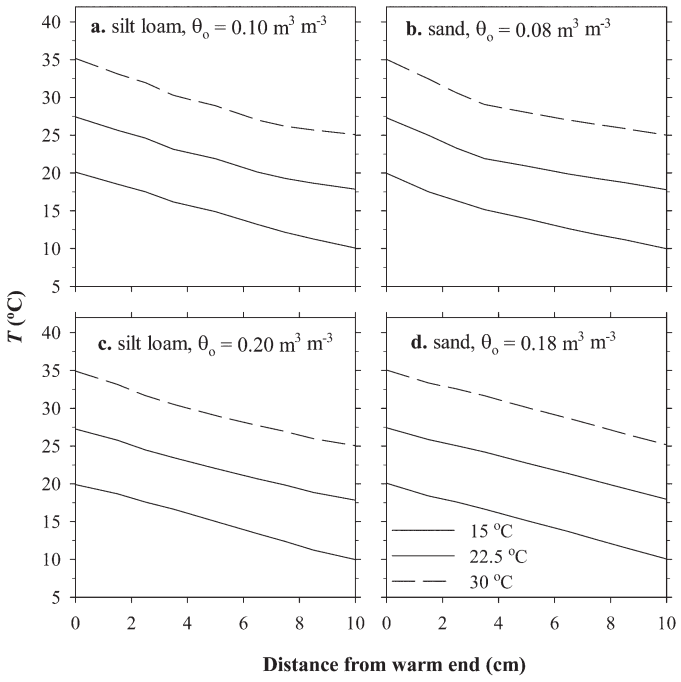

Fig. 4. Steady-state temperature (T) distributions for 100°C m^{-1} temperature gradients. Lines represent temperature distributions obtained after 96-h application of imposed temperature gradients (θ_o = initial water contents).

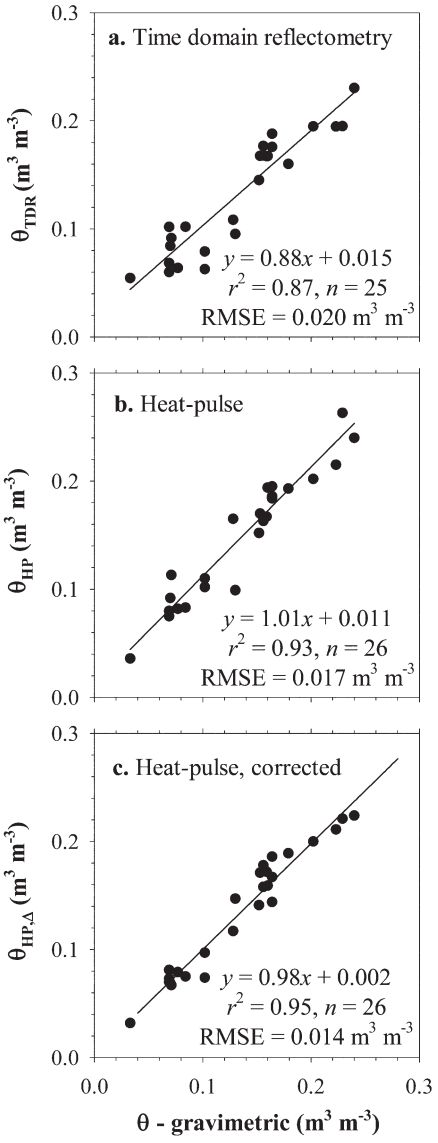

Fig. 5. Regression of thermo-time domain reflectometry-measured water content vs. gravimetric water content (θ): (a) TDR determined θ (θ_{TDR}); (b) heat pulse determined θ (θ_{HP}); and (c) heat pulse measured θ corrected for initial moisture conditions ($\theta_{HP,\Delta}$). The number of points (n) included in the regression is indicated in each panel.

tion of c_s either from Eq. [4] (Basinger et al., 2003) or from measurement with the heat-pulse method (Ren et al., 2003b). The parameter c_s provides offsets in calculation of θ_{HP} rather than bias (Basinger et al., 2003). Consequently, regression of $\theta_{HP,\Delta}$ provided a slightly lower RMSE, a near-zero intercept, and a larger r^2. This approach has also been used successfully by others (e.g., Heitman et al., 2003; Ochsner et al., 2003), but requires knowledge of the initial moisture distribution, which may provide a limitation under some circumstances. Overall, each of the three methods produced valid estimates of θ in these closed column experiments, but for the remainder of the results we report θ computed as $\theta_{HP,\Delta}$.

Comparison of Moisture and Steady-State Temperature Distributions

Moisture redistribution provides a primary mechanism for producing nonuniformity of thermal properties. Evidence of nonuniformity in thermal properties was apparent from the steady-state temperature distributions observed at 96 h (Fig. 3–4). Therefore, θ distributions would be expected to be nonlinear and to have transitions consistent with temperature distributions. Paired moisture and temperature distributions for silt loam (gradient = 150°C m^{-1}, mean = 30°C) and sand (gradient = 150°C m^{-1}, mean = 15°C) are shown in Fig. 6 and 7, respectively. For sil-10, both temperature and moisture distributions show a major shift at 6 to 8 cm from the warm end of the cell (Fig. 6a). The moisture distribution shifts from uniformly low (<0.10 m^3 m^{-3}), with an increase approaching 0.10 m^3 m^{-3}. Similarly, the temperature distribution is approximately linear near the warm end, with a decrease in the magnitude of the slope occurring at 6 to 8 cm. The moisture distribution and consequently thermal properties are nonuniform near the cool end of the column. The impact of this nonuniformity on the temperature distribution is complicated, because heat transfer mechanisms beyond simple conduction are involved. Water vapor was probably moving toward the cold end, where it condenses. Thus, there was a latent heat transfer that decreases the temperature gradient.

For sil-20, temperature distribution shifts are more subtle than sil-10 (Fig. 6b), but can be observed as deviation from the dotted line, which represents a linear temperature distribution. The slope magnitude for the temperature distribution first increases near 2 cm and then decreases near the cell midpoint and becomes constant. Another slight slope shift in the temperature distribution occurs at 7 to 8 cm, where the magnitude of the slope further decreases. Changes in the moisture distribution are apparent in these same regions. A large change in θ (∼0.15 m^3 m^{-3}) occurs from 2 to 5 cm and then a more subtle change in θ occurs at 7 to 8 cm.

The temperature distribution for s-8 showed an inflection point at 3 to 4 cm, with nearly linear temperature distributions before and after the inflection point (Fig. 7a). A major shift in the shape of the moisture distribution is also apparent at 3.5 cm. Moisture content is nonuniform along the cell, but a major shift in the slope of the moisture distribution occurs at 3.5 cm. As mentioned above, the full impact of moisture nonuniformity requires consideration of mechanisms beyond simple conduction; however, major transitions in moisture and temperature distributions have consistent locations. The s-18 cell shows more uniform thermal properties than s-8, with observed θ varying by ≤0.03 m^3 m^{-3} along the cell (Fig. 7b); temperature distributions were also consis-

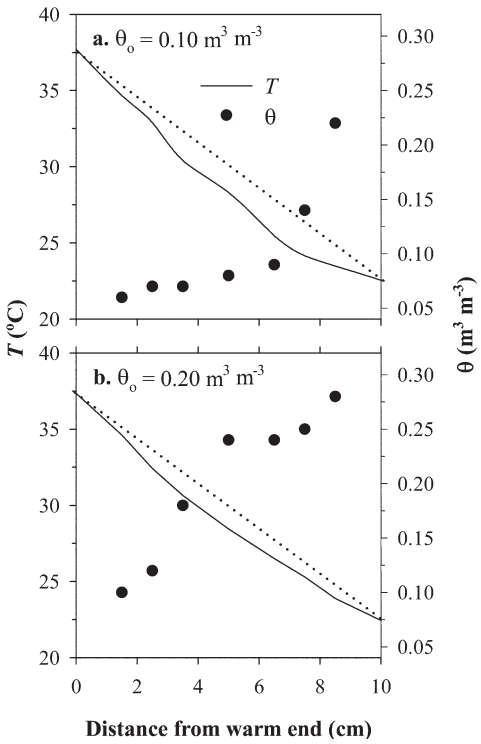

Fig. 6. Paired temperature (*T*) and water content (θ) distributions for silt loam. Plots show conditions after 96 h for 150°C m^{-1} temperature gradient at 30°C mean temperature. The dotted line represents a linear temperature distribution (θ_o = initial water contents).

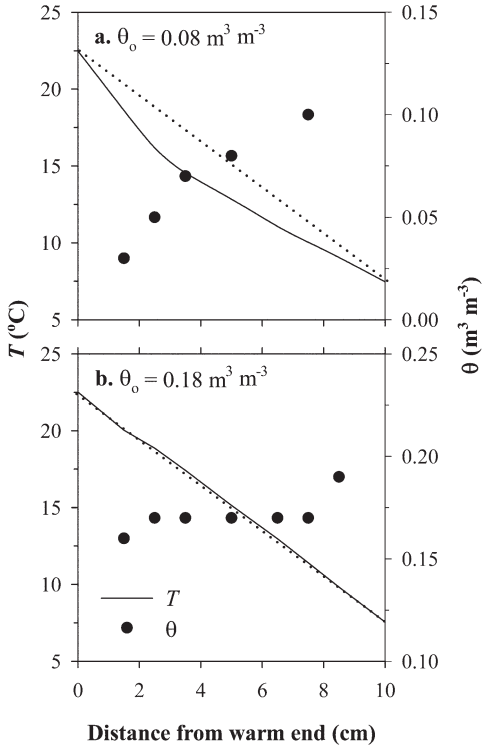

Fig. 7. Paired temperature (*T*) and water content (θ) distributions for sand. Plots show conditions after 96 h for 150°C m^{-1} temperature gradient at 15°C mean temperature. The dotted line represents a linear temperature distribution (θ_o = initial water contents). Note that different θ ranges are plotted in (a) and (b).

tently linear (Fig. 3 and 4). The moisture distribution observed for these conditions was similar to moisture conditions observed for s-18 throughout the experiments as θ varied by ≤0.02 m^3 m^{-3} at a given measurement location. Thus, s-18 probably had little net thermal moisture redistribution.

Thermal Conductivity Distributions

Consistencies in the shapes of one-dimensional temperature and θ distributions provide one means of observing coupled heat and water transfer. The T-TDR sensors, however, provide further utility in that thermal properties can be measured directly and compared with temperature distributions. Soil temperature and λ distributions are shown for sil-10, sil-20, and s-8 in Fig. 8 (corresponding to Fig. 6 and 7a). The s-18 λ distribution corresponding to Fig. 7b (data not shown) had a cell mean of 1.75 W m^{-1} °C^{-1} and varied <0.15 W m^{-1} °C^{-1} from the mean at any measurement location, which is consistent with its near-uniform θ distribution.

For sil-10, λ increased slightly from the cell warm end to 6.5 cm and then shows a large increase. The inflection point location for λ is consistent with the inflection point in the temperature distribution. As suggested above, the shape of the distributions for thermal properties should also be consistent with the θ distribution (Fig. 6a). Since the relationship between λ and θ is nonlinear and unique to a particular soil, direct measurement provides further insight into the influence of λ on heat transfer and the shape of temperature distributions.

Consistency among shapes of the λ, θ, and temperature distributions can also be observed for sil-20 and s-8 (Fig. 6b, 7a, and 8), even though heat transfer in the cells is not due solely to conduction. Despite the influence of θ on λ, the shapes of the λ and θ distributions are not identical (i.e., relative increases in λ differ in magnitude from relative increases in θ). Thus, the capability to directly measure thermal properties (*C*, λ, and thermal diffusivity) with T-TDR offers an opportunity to extend the experimental study of mechanisms for heat transfer beyond what is possible with the measurement of only θ.

Moisture Redistribution

Moisture conditions were transient at 96 h, whereas temperature distributions approached steady state. This complicates direct comparison between θ distributions resulting from sequentially imposed temperature boundaries for the time periods used in these experiments. Thus far, we have chosen to focus our comparison toward the effect of moisture redistribution on temperature, rather than directly comparing θ distributions. The effect of this thermal moisture redistribution on thermal properties is apparent directly from the shape of the λ distributions as well as indirectly from the nonlinear steady-state temperature distributions. To illustrate the transient moisture conditions observed during the experiments, however, we compared θ distributions obtained during five different sequentially imposed boundary conditions for sil-20 (Fig. 9).

The θ distribution appears most uniform for the initial imposed temperature condition of mean = 15°C, gradient = 50°C m^{-1}, but even this shows some net moisture movement away from the warm end of the cell. Moisture redistribution progressed noticeably for mean = 22.5°C, gradient = 50°C m^{-1} and continued to increase for the remaining conditions. Changes in the moisture distribution were more subtle between mean temperatures 22.5 and 30°C for

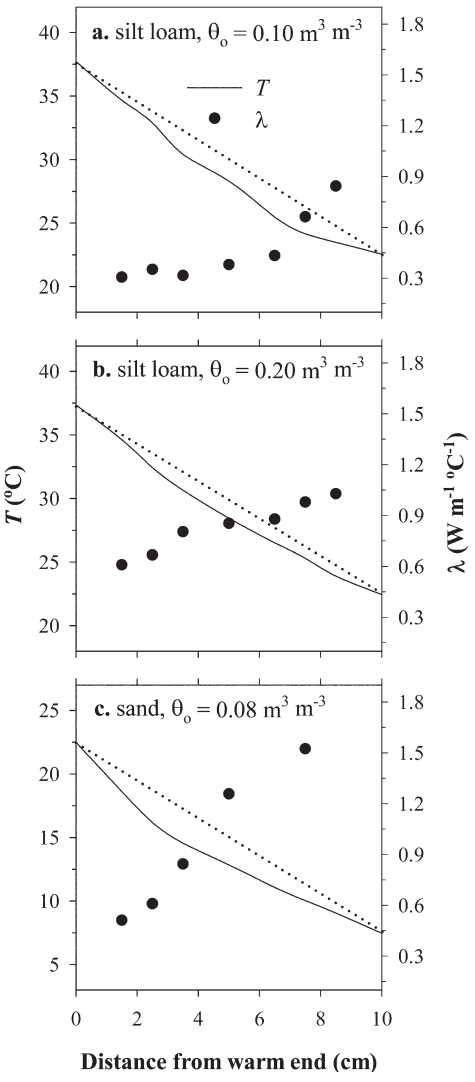

Fig. 8. Paired temperature (*T*) and thermal conductivity (θ) distributions. Plots show conditions after 96 h for imposed boundary temperature conditions corresponding to Fig. 6 and 7a (θ_o = initial water contents). The dotted line represents a linear temperature distribution.

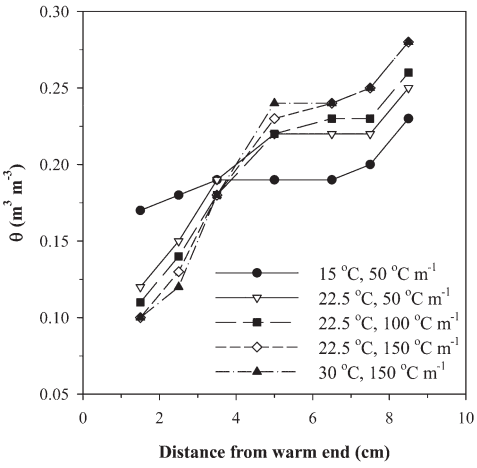

Fig. 9. Transient water content (θ) distributions. Plots show conditions for the silt loam at an initial θ = 0.20 m^3 m^{-3} after 96 h for each imposed temperature condition. Temperature conditions are indicated by the mean temperature, temperature gradient combination.

the 150°C m^{-1} gradient, but are still apparent by the more abrupt change in θ along the cell at distances <5 cm. For reasons given above, we limit extensive comparison. Net moisture redistribution similarly increased during the experiment for sil-10 and s-8, but was minimal for s-18 (data not shown).

From these experiments, there is also some opportunity to compare moisture redistribution for differing θ_o conditions and between soils. As mentioned above, s-18 showed limited thermal moisture redistribution, whereas varying patterns of thermal moisture redistribution were observed for sil-10 (Fig. 6a), sil-20 (Fig. 6b), and s-8 (Fig. 7a.). Yet θ_o for s-18 falls within the range of the remaining three initial moisture conditions. When viewed in terms of air-filled porosity, however, s-18 with 0.21 m^3 m^{-3} air-filled porosity falls well below the air-filled porosity of sil-20 (0.35 m^3 m^{-3}). Air-filled porosity is important to vapor transport. Air-filled porosity was similar for sil-10 and s-8 (0.31 m^3 m^{-3}), yet the shapes of their temperature and moisture distributions differ (Fig. 3, 4, 6, and 7). These differences may be related to their water characteristic relationships (Fig. 1). Matric potential was much lower for sil-10 than s-8, thus restricting water redistribution. This suggests the coupling of both temperature and potential gradients in nonisothermal moisture redistribution.

Transient Temperature, Water Content, and Thermal Conductivity Distributions

Following the application of the first nine temperature gradients, we reversed the direction of the temperature gradient. Conditions were transient throughout the experiment, but this reversal of the temperature gradient provides a more dynamic case to illustrate measurement of transient temperature, θ, and λ distributions, particularly here beginning from a nonuniform moisture distribution. Temperature, θ, and λ distributions for sil-10 and s-8 at 24, 48, and 96 h after this shift are shown in Fig. 10 and 11, respectively.

Time-step comparisons show a net shift in moisture toward the cool end of the cell (formerly the warm end) from thermally driven

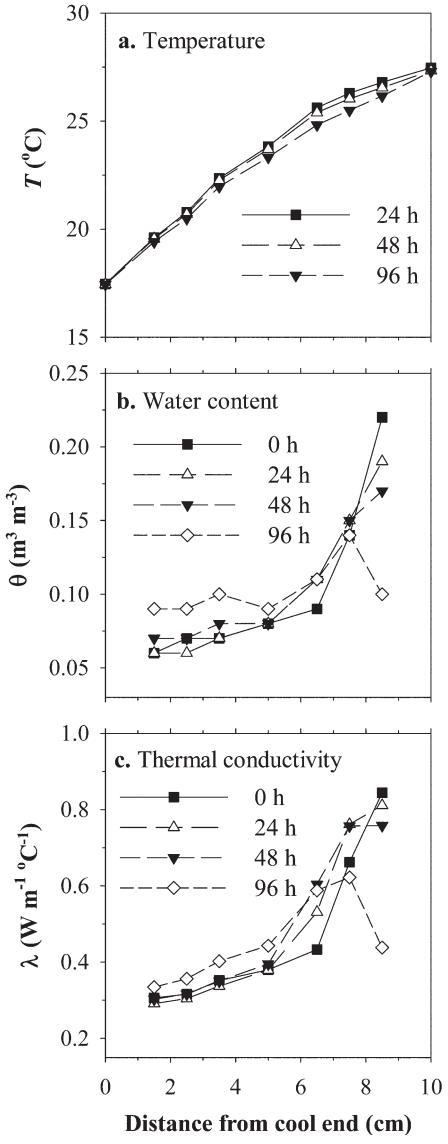

Fig. 10. Temperature (*T*), water content (θ), and thermal conductivity (λ) distributions following reversal of the temperature gradient for silt loam at initial θ = 0.10 m^3 m^{-3}. The temperature gradient direction was reversed at time = 0 h.

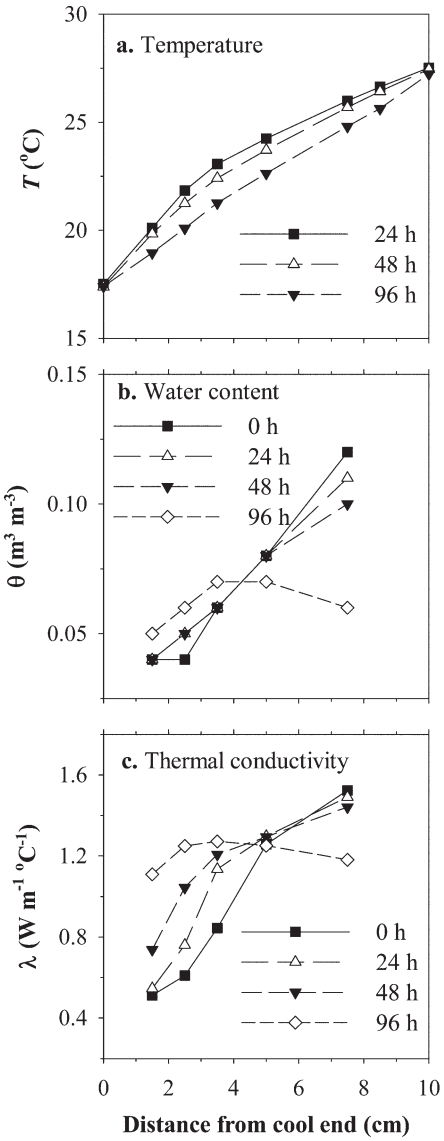

Fig. 11. Temperature (*T*), water content (θ), and thermal conductivity (λ) distributions following reversal of the temperature gradient for sand at initial θ = 0.08 m^3 m^{-3}. The temperature gradient direction was reversed at time = 0 h.

moisture redistribution. Moisture redistribution transfers heat and leads to changes in λ, which can be observed from the shifting temperature and λ distributions. The pattern in these transient distributions differs between sil-10 (Fig. 10) and s-8 (Fig. 11) owing to differences in the initial moisture and temperature distributions, air-filled porosities, water-characteristic relationships, and λ–θ relationships, among others, all of which are important to coupled heat and water transfer. The ability of the instrumented soil cell to capture these changes in short time steps and for the same soil sample provides a new opportunity to study dynamic heat and water transfer processes. Direct knowledge of temperature, θ, and λ distributions during both periods of transient and near-steady-state conditions is possible only with in situ measurement.

CONCLUSIONS

Coupled heat and moisture transfer in soil remains an important topic in need of experimental investigation. Our study implements new techniques for temperature control and in situ measurement that overcome limitations from previous studies by providing one-dimensional conditions along with direct observation of temperature, θ, and λ distributions under transient boundary conditions.

Our results indicate nonlinearity in temperature distributions under a variety of imposed temperature boundaries. This outcome differs from previous work where temperature control was less successfully implemented, but is consistent with nonuniform thermal properties resulting from moisture redistribution under one-dimensional conditions. The use of T-TDR sensors provides several methods for estimating θ, all of which compare favorably with gravimetric measurements. These measured θ and temperature distributions demonstrate consistency through colocated inflection points. The effect of moisture redistribution on thermal properties is further demonstrated through direct measurement of λ by T-TDR. Among the soil–θ_o conditions tested here, we observe little thermal moisture redistribution for sand at high initial moisture, but there are varying patterns of redistribution for the remaining three soil–θ_o combinations. Measurement of θ with T-TDR allows comparison of these θ distributions under a series of imposed boundary conditions for the same soil sample. Further, the use of T-TDR allows observation of temperature, θ, and λ distributions under more dynamic conditions, as we demonstrated with a reversed temperature gradient.

These experiments demonstrated new techniques for the study of coupled heat and water transfer under temperature-controlled, instrumented laboratory conditions, which extend previous experiments. Improved temperature control allows comparison of temperature and θ distributions under one-dimensional conditions. Implementation of T-TDR provides the opportunity for direct observation of both θ and λ during transient and near-steady-state conditions under multiple imposed temperature conditions on the same sample. These techniques allow improved investigation of mechanisms involved in coupled heat and water transfer. The successful use of T-TDR for in situ measurement of θ and thermal property dynamics also envisages new opportunities to extend work to field conditions where temperature, θ, and thermal properties are predominantly transient.

ACKNOWLEDGEMENTS

The research in this journal paper of the Iowa Agric. and Home Econ. Exp. Stn., Ames, IA, was supported by the National Science Foundation under Grant No. 0337553 and by Hatch Act and State of Iowa Funds.

REFERENCES

Bach, L. 1992. Soil water movement in response to temperature gradients: Experimental measurements and model evaluation. Soil Sci. Soc. Am. J. 56:37–46.

Basinger, J.M., G.J. Kluitenberg, J.M. Ham, J.M. Frank, P.L. Barnes, and M.B. Kirkham. 2003. Laboratory evaluation of the dual-probe heat-pulse method for measuring soil water content. Vadose Zone J. 2:389–399.

Bristow, K.L., G.S. Campbell, and K. Calissendorff. 1993. Test of a heat-pulse method for measuring changes in soil water content. Soil Sci. Soc. Am. J. 57:930–934.

Bristow, K.L., G.J. Kluitenberg, and R. Horton. 1994. Measurement of soil thermal properties with a dual-probe heat-pulse technique. Soil Sci. Soc. Am. J. 58:1288–1294.

Cahill, A.T., and M.B. Parlange. 1998. On water vapor transport in field soils. Water Resour. Res. 34:731–739.

Campbell, G.S., C. Calissendorff, and J.H. Williams. 1991. Probe for measuring soil specific heat using a heat-pulse method. Soil Sci. Soc. Am. J. 55:291:293.

Dane, J.H., and J.W. Hopmans. 2002a. Pressure cell. p. 684–688. *In* J.H. Dane and G.C. Topp (ed.) Methods of soil analysis. Part 4. Physical methods. SSSA Book Ser. 5. SSSA, Madison, WI.

Dane, J.H., and J.W. Hopmans. 2002b. Pressure plate extractor. p. 688–690. *In* J.H. Dane and G.C. Topp (ed.) Methods of soil analysis. Part 4. Physical methods. SSSA Book Ser. 5. SSSA, Madison, WI.

Heitman, J.L., J.M. Basinger, G.J. Kluitenberg, J.M. Ham, J.M. Frank, and P.L. Barnes. 2003. Field evaluation of the dual-probe heat-pulse method for measuring soil water content. Vadose Zone J. 2:552–560.

Kluitenberg, G.J. 2002. Heat capacity and specific heat. p. 1201–1208. *In* J.H. Dane and G.C. Topp (ed.) Methods of soil analysis. Part 4. Physical methods. SSSA Book Ser. 5. SSSA, Madison, WI.

Nassar, I.N., and R. Horton. 1989. Water transport in unsaturated salty soil: I. Experimental results. Soil Sci. Soc. Am. J. 53:1323–1329.

Noborio, K., K.J. McInnes, and J.L. Heilman. 1996. Measurement of soil water content, heat capacity, and thermal conductivity with a single TDR probe. Soil Sci. 161:22–28.

Ochsner, T.E., R. Horton, and T. Ren. 2003. Using the dual-probe heat-pulse technique to monitor soil water content in the vadose zone. Vadose Zone J. 2:572–579.

Or, D., B. Fisher, R.A. Hubscher, and J. Wraith. 1998. WinTDR 98 Version 4.0: User's guide. Utah State Univ., Logan.

Prunty, L., and R. Horton. 1994. Steady-state temperature distribution in nonisothermal, unsaturated closed soil cells. Soil Sci. Soc. Am. J. 58:1358–1363.

Ren, T., Z. Ju, Y. Gong, and R. Horton. 2005. Comparing heat-pulse and time domain reflectometry soil water contents from thermo-time domain reflectometry probes. Vadose Zone J. 4:1080–1086.

Ren, T., K. Noborio, and R. Horton. 1999. Measuring soil water content, electrical conductivity, and thermal properties with a thermo-time domain reflectometry probe. Soil Sci. Soc. Am. J. 63:450–457.

Ren, T., T.E. Ochsner, and R. Horton. 2003a. Development of thermo-time domain reflectometry for vadose zone measurements. Vadose Zone J. 2:544–551.

Ren, T., T.E. Ochsner, R. Horton, and J. Zu. 2003b. Heat-pulse method for soil water content measurement: Influence of the specific heat of the soil solids. Soil Sci. Soc. Am. J. 67:1631–1634.

Soil Survey Staff. 1972. Soil survey laboratory methods and procedures for collecting soil samples. Soil Surv. Invest. Rep. 1. U.S. Gov. Print. Office, Washington, DC.

Topp, G.C., J.L. Davis, and A.P. Annan. 1980. Electromagnetic determination of soil water content: Measurements in coaxial transmission lines. Water Resour. 16:574–582.

Welch, S.M., G.J. Kluitenberg, and K.L. Bristow. 1996. Rapid numerical estimation of soil thermal properties for a broad class of heat pulse emitter geometries. Meas. Sci. Technol. 7:932–938.

Zhou, J., J.L. Heitman, R. Horton, T. Ren, T.E. Ochsner, L. Prunty, R.P. Ewing, and T.J. Sauer. 2006. Method for maintaining one-dimensional temperature gradients in closed, unsaturated soil cells. Soil Sci. Soc. Am. J. 70:1303–1309.